International Journal of Manufacturing, Materials, and Mechanical Engineering
Volume 12 • Issue 1

Island-Matrix Inhomogeneous Deformation Behavior, Formation of Deformation Band, and BUT Forming of DP Steel

Amit Kumar Rana, The ICFAI University, Tripura, India*
Partha Pratim Dey, Indian Institute of Engineering Science and Technology, Shibpur, India

ABSTRACT

Islands-matrix-dual-phase (I-M-DP) steel has received a great deal attention for better concern with the emissivity, fuel consumption, and passengers safety. A number of deformation plasticity issues are yet to be fully understood. Complex deformation stages for various stain is predicted as the natural outfall of the plastic strain localization caused by the ill-assorted deformation between the martensite-island phase and the ferritic-matrix phase. Modeling is carried out both in macro level by bending under tension (BUT) for different roller radius/sheet thickness ratios to acquire strain and stress state deformation and micro scale by representative volume element (RVE) according to element position. It can relate both the 2D, 3D micro, and macro-scale finite element-based BUT models' result of flow behavior. Systematically, strain-based severe deformation pattern arises from outfall of plastic strain localization and von Mises stress distribution in island-matrix steels are investigated on the microstructure by finite element method for ill-assorted deformation between phases.

KEYWORDS

Bending-Under-Tension, Island-Matrix DP Steel, Plastic Strain Localization, Representative Volume Element, Severe Deformation Behavior

1. INTRODUCTION

Islands-Matrix-Dual-phase steel (I-M-DP steel) is a high-strength steel that has ferrite as a soft-matrix and hard martensite-islands combined microstructure. The microstructure of dual phase steel consists of ferrite and martensite phases, where ferrite is a matrix and martensite is an island. The processing of Islands-Matrix-Dual-phase steel is done by quenching followed by intercritical annealing (Krajewski and Nowacki, 2014; Darabi et al., 2017; Belgasam and Zbib, 2018). Application in crash-relevant components of vehicle bodies I-M-DP steels are given the high energy absorption capacity (Paul and Kumar, 2012; Belgasam and Zbib, 2018), demanding a combination of strength-ductility, tensile properties (Paul and Kumar, 2012; Paul, 2013) and fatigue properties (Paul et al., 2015a,b; Rana et al.,2019a) of binary phases dual phase steels are particularly well suited for automotive structural and safety parts such as longitudinal beams, cross members and reinforcements. The use of this

DOI: 10.4018/IJMMME.299062 *Corresponding Author

type of steel is not only increasing in the automobile industry but is also aiming towards a better group of high ductility and strength which is further needed with the decrease in vehicle weight, so that fuel consumption also can be reduced. In view of that, car and steelmakers are concerned in detailed forecasting the effect of various microscopic factors as well as optimizing microstructural properties for the application in crash-relevant components of vehicle body's material as I-M-DP steel (Sirinakorn et al., 2014; Belgasam and Zbib, 2017). During the processing route of I-M-dual phase steels, non-metallic inclusions may exist in steel microstructure (Uthaisangsuk et al., 2011). Rana et al., 2019b investigated the outfall of stress field mechanisms using a numerical model due to isotropic elastic inhomogeneity in structural metal under uniaxial tensile stress for soft and hard-inclusions in a matrix. The flow behavior of the I-M-DP steel is utterly dependent on the microstructure parameters. Volume fraction (VFs) and grain sizes (GS) of different phases are also played an important contribution in the mechanical properties of such steel (Paul et al., 2015). Such steel sheets are used in automotive inner panels and body-in-white components which are further required for the design flexibility with respect to various parametric considerations (Paul and Kumar, 2012). Nevertheless, steel suppliers strive to further enhance the mechanical properties of Islands-Matrix-dual phase steels by optimizing their microstructure. Binary phases steels with different grades can be produced by controlling intercritical temperature and the compositions of the constituent (Krajewski and Nowacki, 2014; Belgasam and Zbib, 2018). According to Uthaisangsuk et al., 2011 and Samei et at., 2014 in experiments, concurrently two failure modes were found one cleavage and another dimple fracturing. The de-bonding of the island from ferritic-matrix or the island cracking was formed in the form of void nucleation. On other hand, plastic deformation starts at matrix grains. Hence, the state of yielding initiation of islands-matrix-dual phase steel is mainly governed by the matrix properties. At the time of plastic deformation initiation in the matrix of dual-phase steel, other phase islands that time shows elastic deformation until the overall strain of the material reaches further at a certain level (Paul and Mukherjee, 2014; Zhuang et al., 2014). Carden et al., 2002 determined the failure mechanisms and ductility of the I-M-DP steel with edge crack under different manufacturing conditions.

The common method for the formability test of sheet materials is Bending Under Tension (BUT). BUT experiments have been thoroughly considered by various authors (Li et al., 2002; Wang et al., 2005; Wagoner and Li, 2005). Authors considered many parameters like the velocity of the sheet metal, back tension, bend radius, sheet thickness, etc. for spring back effect via BUT set up. There are three stages of the draw-bend test of a rectangular sheet along its length parallel to the rolling direction. Initially, it involves bending the flat sheet for conforming to the tool with 90° of contact. A proper back force from restraint is applied to the strip, and the strip is drawn over a non-rotating tool at a constant speed (Li et al., 2002; Wang et al., 2005; Wagoner and Li, 2005). In the current study, the failure condition of I-M-DP steel is predicted as the natural outfall of plastic strain localization resulting from the incompatible deformation between the islands and matrix phases. Also, the flow behavior, S Mises stress distribution, and plastic strain localization are investigated for bending under tension forming of I-M-DP 600 steel.

2. FE MODELING

2.1 Micromechanical Approach Using 2D and 3D RVE

In the case of microstructure features of the Islands-Matrix-Dual phase (I-M-DP) steel material is presented in a model based on finite element (FE) through a representative volume element (RVEs). An RVE represents a representative microstructure of the material, which carries general characteristics of the total microstructure and is thought to be homogeneous individually. The results of the investigative study based on RVE should describe the properties of each phase and overall microstructure. Different steps are involved in the modeling of flow behavior using the 2D and 3D-RVEs. The steps are involved such as i) definition of RVEs ii) definition of flow behavior in the

individual I-M phases iii) boundary conditions for predicting the severe deformation characteristics and iv) consideration of homogenization conditions. An RVE carries the essential features of the total microstructure in the microscale. A suitable RVE should be sufficiently large that it can have an average of the microstructural parameters of the whole microstructure but on the other hand, it must be as small as possible so that it can be considered homogeneous throughout for better approximation of stress and strain field. A compatible smaller RVE is also required fewer resources for computation. The advantages of micromechanical modeling using the RVE can be provided a detailed description of the stress and strain dispersion and their evolution in the microstructure during a metal forming process (Liedl et al.,2002; Ajmal, 2009; Paul, 2013; Rana et al., 2020). Images obtained from metallographic tests can be converted into a representative volume element model like QR bar code by using FE software Abaqus. The images from the actual microstructure can be transformed into the 2D RVE model for the preparation of finite element simulation of different deformation processes. Some examples of 2D RVE based on real microstructural features were generated by Paul and Kumar, 2012; and Sodjit and Uthaisangsuk, 2012.

In order to improve veracity in the modeling, 2D RVE has been upgraded towards simplified 3D RVE where islands are randomly dispersed. The second phase particles which are considered as inclusions are dispersed in a matrix (pliable phase). The percentage of pliable matrix and island is considered according to their actual VFs of the microstructure. The 3D RVE is constructed with arbitrary dispersion of pliable-ferrite and island in microstructure, where effects of microstructural interphase boundary layer have not been taken into account in the present simulation as it is insignificant (atomic sizes) compared to the RVE. Paul, 2013 investigated the 2D and 3D RVEs based models of I-M-dual phase steels to predict their flow behavior. Ramazani et al., 2013 reported the optimum size of RVE is concerned with the prediction of the flow behavior of I-M-DP steel using 2D and 3D RVE models. It is also found that 3D modeling of I-M-DP steel provides a better description compared with 2D model flow curve prediction. Uthaisangsuk et al., 2009 also studied mesh size sway on 2D and 3D RVEs models of I-M-DP steel to check the range of the affecting parameters. The following are the key highlights that relate directly to the current study: i) presently RVEs methods are increasingly used for microstructure modeling. ii) Due to the combined effect of matrix and island, I-M-DP steels exhibit a unique combination of strain hardening, strength, and ductility. As a consequence, I-M-DP steels are widely applied in automobile components: such as car body panels, structural members, wheel disks, bumpers, etc iii) The strength of the I-M-DP steel is depending on various parameters influenced on each phase iv) Bending-Under-Tension (BUT) is commonly used method to check the formability of sheet metals. The key material properties of matrix and island phases of I-M-DP steel are taken from Wei et al., 2015 work.

In the present micromechanical-based FE model of I-M-DP steel, von Mises yield criteria (S, Mises), the associative flow rule, and the isotropic hardening rule are assumed for every single phase. To illustrate the isotropic hardening behavior in each entity for the calculations, RVEs model based on dislocation theory (Paul, 2013; Rana et al., 2018) was used. Equation (1) shows the correlation which was used to elucidate the mechanical behavior of matrix and island phases, which is shown in Fig.1:

$$\sigma^{m,i} = \sigma_{y}^{m,i} + \alpha MS\sqrt{b}\sqrt{\frac{1-\exp(-Mk_{r}\varepsilon)}{k_{r}L}}^{m,i} \tag{1}$$

Here stress ($\sigma^{m,i}$) is at a true strain of an ε. Other specified material constants of this model are composed of a previous study (Paul, 2013; Rana et al., 2018).

The foremost term expression of the above equation (1), is the yield stress and total contributions are friction stress, solid solution strengthening, precipitation strengthening with Nb, Ti and/or V, GS, describe as:

$$\sigma_y^{m,i} = 70 + 37wt.\ \%Mn + 83wt.\ \%Si + 2918wt.\ \%N_{sol} + 33wt.\ \%Ni - 30wt.\ \%Cr + 680wt.\ \%P + 38wt.\ \%Cu + 11wt.\ \%Mo + 5000wt.\ \%C + \frac{15.1}{\sqrt{d}} \quad (2)$$

where the above first term is friction stress and the value is 70.0 MPa, and d (GS) is in mm.

The next term parameters that are considered for matrix and island in the RVEs simulation, are tabulated in table 1. From the eq. (1) and eq. (2) the flow curve of the matrix and island can be determined. Plastic properties for the islands and matrix are shown in Fig. 1.

Table 2 shows the chemical components of I-M-DP600 steel in weight percentage (Wei et al., 2015). A quantity of the key advantages of the I-M-DP steels comprises their better-quality strength-ductility properties in comparison with standard steels, moderate price due to the small amount of alloying add-ons, as well as excellent crashworthiness properties. Microstructure-based FE modeling of bending under tension I-M-DP steel sheets under convenient boundary conditions (BCs) requires modeling the entire specimen and within the microstructure. In theory, it is possible to carry out microstructure-based FE modeling of the selected element in the entire specimen. The 2D RVE modeling of the material microstructure in a micro-level area but large enough to capture nucleation

Figure 1. Stress-strain behavior of island-matrix (I-M) steel

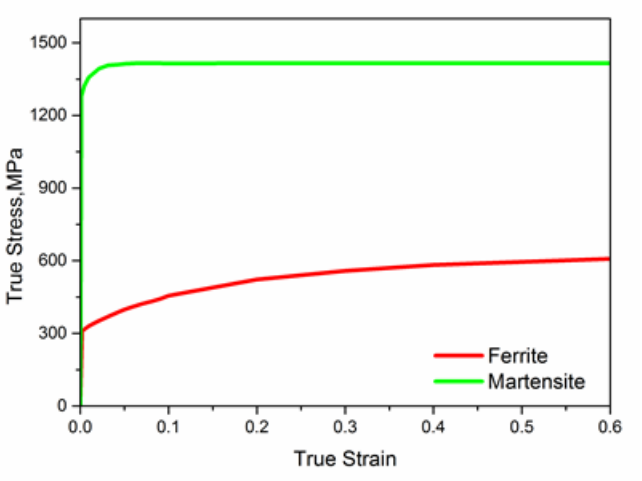

Table 1. Various materials parameters (Paul, 2013; Rana et al., 2018)

Parameters	Symbols	Magnitude(units)
Taylor constant	α	0.33
Taylor factor	M	3
Shear modulus	S	80,000 MPa
Burger's vector	b	2.5×10^{-10} m
Recovery rate in matrix	k_r	$10^{-5}/d_\alpha$
Recovery rate in island		41
Dislocation mean free path for island	L	3.8×10^{-8} m

and coalescence of micro-cracks and severe deformation characteristics in micro and macro levels of the specimen is shown in Fig. 2.

As can be seen in Fig. 3, the generated shape of RVEs of I-M-dual phase steel is cubic. It has been considered a ferritic phase as a matrix and island as a hard inclusion. The numbers of matrix and island were determined according to the phase VFs in the I-M-dual phase steel. The predictive capacity of the model is determined by the selection of Representative Volume Elements (RVEs), and the constitutive laws of phases and the boundary conditions.

To reduce the computational cost, homogenization boundary conditions have been used for a micromechanical modeling, and it is reported to work reasonably well in simulating the tensile behavior of I-M-DP steels (Uthaisangsuk et al., 2009; Sodjit and Uthaisangsuk, 2012; Paul, 2013; Ramazani, 2013; Wei et al., 2015; Rana et al., 2018; Dai et al., 2020). However, the RVEs generated by matrix and islands, have the advantages in revealing the effect of the real microstructure morphology and the onset of strain localization, which is important to the failure analysis.

2.2 Macroscopic FE Modeling of BUT Setup

The BUT model, which is used here for an I-M-DP 600 strip that Wagoner and Li, 2005, was introduced in his literature. It was a type of spring backtest. It is particularly important for the parts where one or two dimensions are much larger than the remaining ones, such as in a sheet metal part. This strip is divided into three parts, two rectangular parts along with a curve bending part as shown in Fig 4. In case of the macro modeling, all dimensions are considered in mm. The thickness (t) of the strip is 1.2 mm. Strips are made with three different bending ratios 6.7, 16.7, and 20.8. The bending radius(r) for the strips is 8 mm, 20 mm, and 25 mm. The island elements are shown using grey color and matrix elements are shown using dark green color. Individual sets of matrix and island are shown in Fig 4.

Figure 2. Distinct Set of phases in 2D RVE a) matrix set b) island set c) I-M-DP 600

Figure 3. 3D RVE details of I-M-DP 600 steel

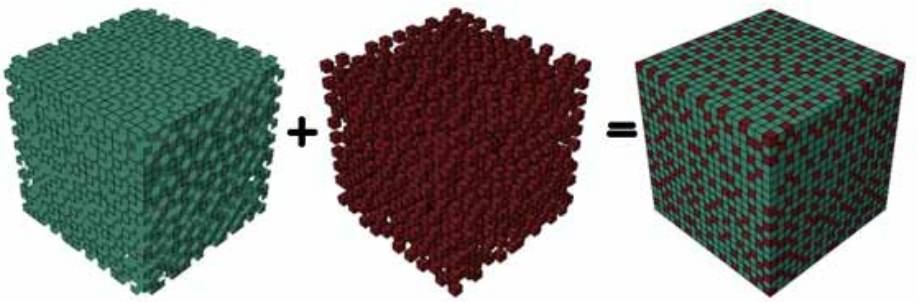

Table 2 Main chemical components of the investigated steel in weight %

Steel	C(%)	Si(%)	Mn(%)	P(%)	Cr(%)	Mo(%)	Al(%)	V(%)
I-M-DP600	0.124	0.066	1.33	0.0069	0.013	0.154	0.827	0.0025

Figure 4. 3D BUT details of I-M-DP 600 sheet a) matrix set b) island set c) island-matrix

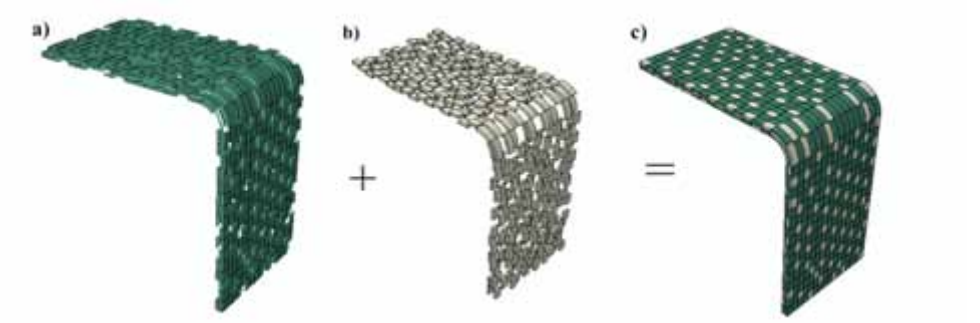

After the application of the properties, the roller and the strip are assembled with dependent instant types. Then a new step is created which is static and general. For this analysis, the Nlgeom is taken into consideration. Interaction between the roller and the strip is taken as tangential behavior, and the frictional properties are neglected. Contact between the strip and the roller is general surface to surface contact in which one of the surfaces is taken as the master surface. The structure of mesh was hex-dominated, and the open technique was used in beneath of mesh controls.

For meshing of BUT model, C3D8R (8-noded brick, reduced integration, hourglass control) is used for discretization of bending sheet. In the BCs of the I-M-DP steel sheet, the upper end is constrained in X, Y, and Z – paths with respect to back stress, and on the other end of the strip is given displacement concerning the velocity, as shown in Fig. 5. Thus, all the degrees of freedom are constrained for the nodes located on the fixed arm. On the other hand, the boundary condition (BCs) is provided to the roller so that it can only roll around the rolling path in its axis, not to displace along any of the axes.

3. RESULT AND DISCUSSION

A materialized approach for weight reduction of a vehicle body is considered to make the most of thinner steel sheet, at the same time as maintaining safety criteria. This eventuating method requires a good design of strength and ductility for meeting crashworthiness and metal forming processes criteria. The uniaxial tensile flow behavior of the investigated I-M-DP600 steel is shown in Fig.6. I-M-DP600 steel can be considered for the typical automotive wheel disc and is a passenger car wheel disc. A typical automotive wheel disc is one of the most severely stressed mechanism regions in the vehicle, and its durability is of vital importance to human safety (Das et al., 2020). Hence, this study aims to FE simulation results to examine the effect of the severely stressed mechanisms in the prediction of BUT condition in the I-M-DP steel sheet. The state of stress-strain is determined at a location of the sheet by FE simulation after incorporating bending ratios variation and hence tensile plasticity. The thickness of the strip is 1.2 mm. Strips are made for three different bending ratios (r/t) 6.7, 16.7, and 20.8. The bending radii for the roller are 8 mm, 20 mm and 25 mm respectively.

Stress and strain analysis of the model is done for all the above-mentioned bending ratios, and stress and strain localization is investigated. Similarly for micromechanical simulation, different

Figure 5. Schematic of 3D-Model with parameters

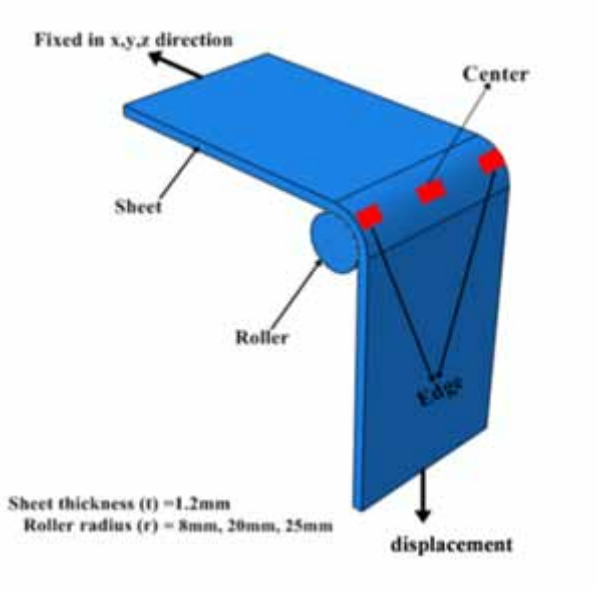

displacements control are used to investigate the flow behavior and plastic strain dispersion of I-M-DP 600 steel, and also its distinct phases (matrix and island) strain partitioning effect on deformation is examined. Figure 6 shows that the experimental flow curve obtained from the literature (Wei et al., 2015) matched well with the simulation in an engineering safe design sense.

3.1 Macroscopic FE Simulation on BUT

Sheet metal-formed structural component is widely used in automobile body and structure. As a product, in the past few years, a large amount of research has been devoted to the development of high

Figure 6. Characteristics of the flow behavior of RVEs (2D and 3D) and BUT simulations with experimental results

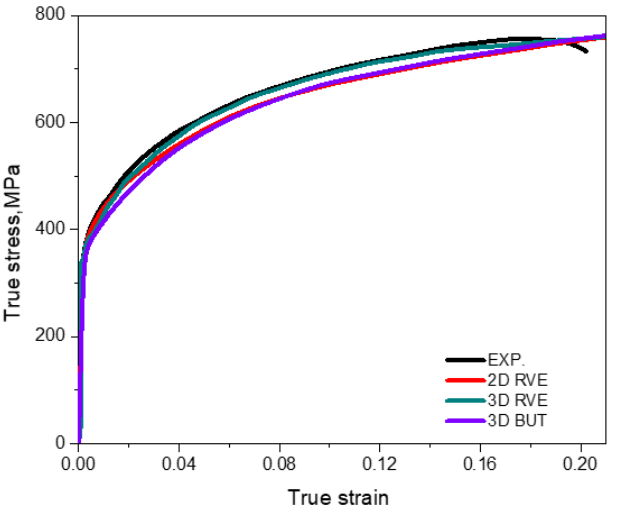

strength steels for automotive structure, body, and wheel applications, which can provide a potential replacement for the conventionally used mild steel (MS). An isotropic hardening with an S, Mises yield criteria was used for the study. Equivalent von-Mises Stress and plastic equivalent strain for BUT model with r/t ratios 6.7, 16.7, and 20.8 are examined.

Though the von-Mises stress value for various bending ratios is almost equal if compare to the value of only matrix phases then it decreases with the increase in bending radius as the strip thickness is fixed. It is also seen from the simulation results in Fig. 7 that the change in bending ratio causes a drastic change in a plastic equivalent strain which decreases with the increase in bending ratio. From the result, it can be seen that islands provide the strength for the material, and the ductile plastic properties are mainly dependent upon the ferritic matrix. Comparing the results from the simulation with the varying r/t ratio, it is seen that the dominant stress in the ferritic matrix decreases from 556.0 MPa to 472.9 MPa due to an increase in bending radius of I-M-DP steel sheet which will decrease the chances of more ductile failure of a sheet at a higher bending radius. Results also indicate the high sensitivity of matrix particles constrained by the island towards the bending ratios which can be helpful in the initial stage of formation. The result can be used as a reference for the development work of sheet metal forming of I-M-DP steel in the automotive industry. Figures 7, 8, and 9 clearly show that the macro modeling results of the equivalent plastic strain vary with a rise of bending ratio.

Figure 7. BUT model simulation for r/t ratio 6.7 (a-c) equivalent von Mises stress (d-f) plastic equivalent strain on overall, matrix and island respectively

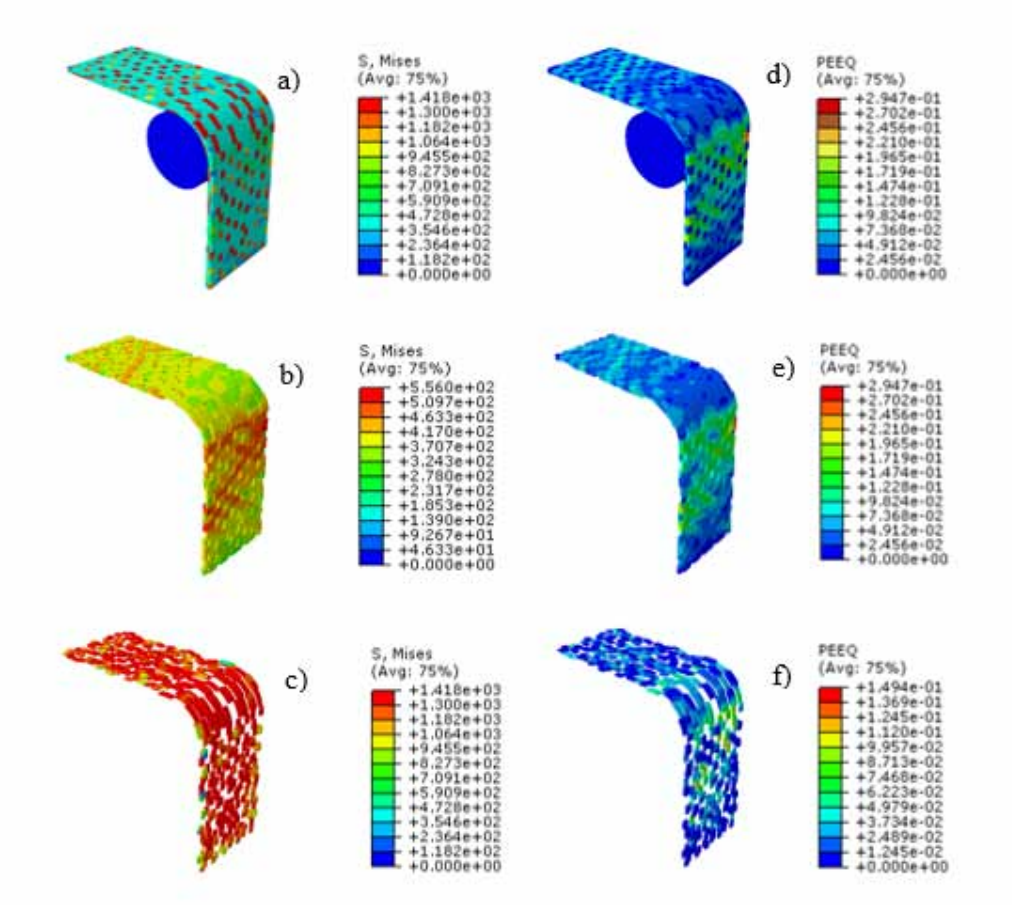

Figure 8. BUT model simulation for r/t ratio 16.7 (a-c) Equivalent von Mises stress (d-f) Plastic Equivalent Strain on overall, in matrix and island respectively

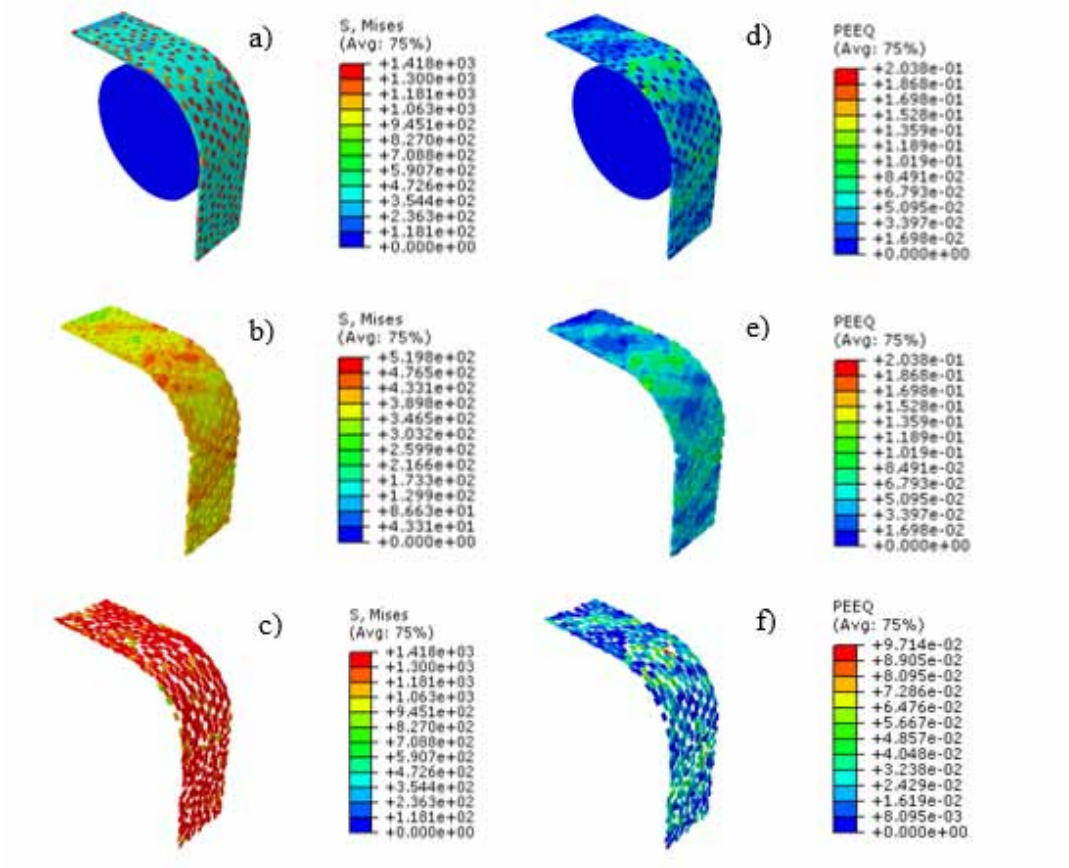

The observed deformation characteristics indicate that initially load has been transferred from matrix to island through the interface and strain has been accumulated on the matrix in the early stage of plastic deformation due to disparities of the morphology of the two phase's I-M-DP steel. The phenomenon of strength and elongation ratio may have significant implications for manufacturing and industrial forming processes, where complex or unpredictable characteristics and part shapes are obstacles to consistent assembly and product quality. Interpretation of deformation mechanisms of DP steel, however, is very difficult because stress and strain vary continuously through the specimen thickness at all stages of deformation and plastic strain localization which arises due to incompatible deformation between the island and soft matrix phases. But these binary phases I-M-DP steels have received a great deal of application due to their handy combination of high strength, high work hardening rate, and ductility. Even though the islands are manifested a significant consequence on strain hardening of I-M-DP steels, the island behavior generally evinces elasticity unless deformation reaches a high-stress level.

3.2 Microscopic Simulation on 2D RVEs

To get the assessment or result instead of analyzing the whole specimen there can be used an RVEs which is the fundamental volume element, over which an evaluation or analysis has been made that will yield a significance that represents the whole. In case of two phase's I-M-DP steel, the model

Figure 9. BUT model simulation for r/t ratio 20.8 (a-c) Equivalent von Mises stress (d-f) Plastic equivalent Strain overall, matrix and island respectively

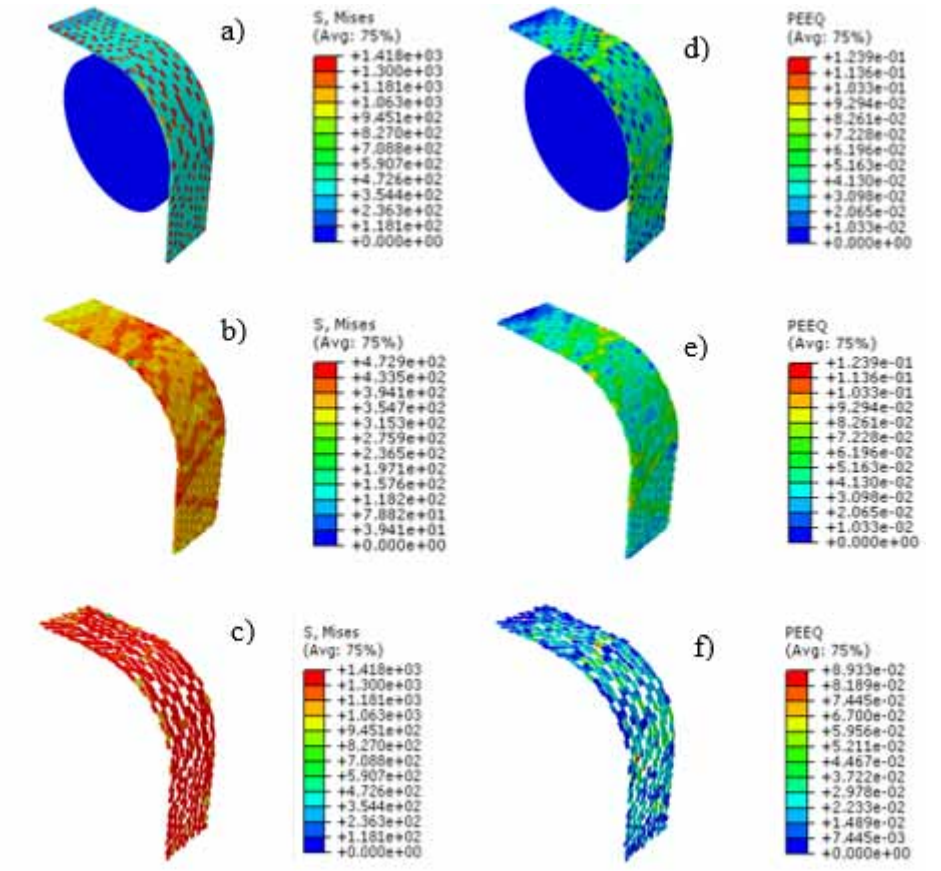

has been created by the selection of periodic representative volume in a random media. The RVE of I-M-DP 600 steel is modeled in respective phases by volume fraction in which the matrix (76.5%) and island (23.5%) are present. To perform the RVE analysis, ABAQUS or CAE "Complete Abaqus Environment" is used. The micromechanical modeling sets of matrix and island phases are depicted in Fig. 2 (a-c). Figure 3 depicts matrix set, island set, and the overall I-M-DP600 for 3D RVE. The material properties used for micromechanical 2D and 3D RVE simulation are the same as those used in bending under tension test simulation. The perfect bonding between matrix and island is considered via. FE simulation. Both phases are following S, Misses elastic-plastic material law; dislocation theory was used to define the isotropic flow behavior of each phase. No separate damage law/failure criteria are incorporated in the FE-based RVE simulations. The approach manifested the flow behavior of I-M-DP steels using virtual tension tests with an RVE to root the significant mechanical fields. In this RVE simulation change in microstructure was analyzed by strain control for the overall straining i.e. 5%, 10%, 15%, 20%. In the present study, displacement control was used as the loading method. Recent studies have manifested the transformation of strain rate on the plastic state of I-M-DP steels under both quasi-static load settings. As shown in Fig. 10 which is extracted RVEs boundary conditions of edge and center position from the actual BUT model.

For both positions, the plane strain modeling procedure is adopted during FE analysis as the width of the tensile sample is much larger than the thickness. For the center position, no lateral boundary

Figure 10. Extraction of (a) edge and (b) center portion RVE from BUT model

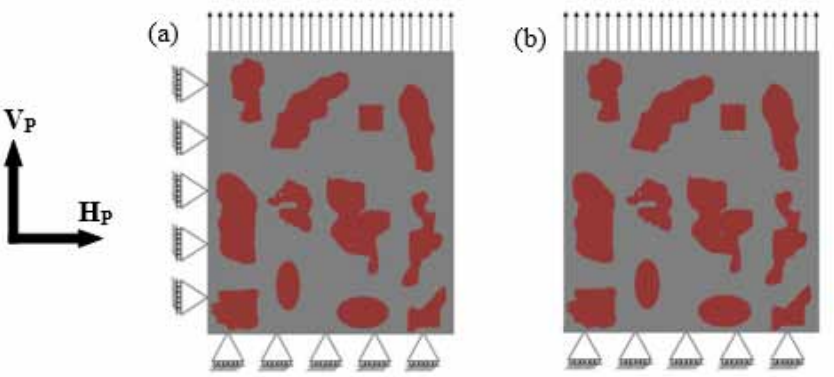

condition is defined but for the edge portion one side is assigned with lateral boundary condition and the other is left free hence the load setting of the specimen. Because one lateral side of the edge region, close to the free boundary of the specimen, can be considered to have no constraint along the rolling direction. At the center of the specimen, the stress state can be considered to be under plane strain with no lateral constraints because the width of the sheet specimen is much larger than its thickness. Since the RVEs are assumed to be the representative in-plane microstructure for the I-M-DP steel under examination. For both the positions, all the nodes on the top edge of the RVE are given the same displacement in V_p path. The displacement boundary conditions that are applied to the RVE edge region are shown in Fig. 10(a) and the boundary condition applied to the centre region is shown in Fig. 10(b). For the edge position, all the base nodes are fixed in V_p path and the left nodes are constrained in H_p path but are free to move in V_p path. For centre position only the base nodes are fixed in V_p path and varying displacement is given on all the upper edge nodes of the RVE. For meshing of selected RVE under element type plane strain element was adopted with reduced integration technique with hourglass control i.e. CPE4R: A 4-node bilinear plane strain quadrilateral, reduced integration, hourglass control.

The average engineering strain in the V_p path is obtained by dividing the displacements of the base edge with the initial length of this model. Average engineering stress is obtained by the reaction force of the 2D RVE in the V_p path divided by the initial cross-sectional area. Finite element computations are conducted on ABAQUS to examine the severe deformation modes of the binary phase's I-M-DP steel under the different BCs representing the two positions "Edge" and "Centre" on bending under the test sample. A typical deformation behavior of 2D RVE element with BCs for edge position like Fig. 10(a) and centre position like Fig. 10(b) is predicted by microstructure level inhomogeneity in the form of plastic strain distribution.

During loading the effect of deformation on I-M-DP600 steel, various displacements are controlled on the RVE. The real microstructure of I-M-DP600 steel comprises 76.5% ferritic-matrix and 23.5% martensite-island and hence the same phase volume fractions are modeled in the present RVEs. A systematic study was performed for different engineering strains i.e. 5%, 10%, 15%, and 20% straining. The equivalent S, Mises stress, and the plastic equivalent strain on the overall, matrix and island of I-M-DP steel are depicted in Fig.11 and 12 for edge position. The equivalent S, Mises stress, and the plastic equivalent strain on the overall, matrix and island are shown in Fig.13 and 14 for the middle position. The following section comprises the simulation results of the microscopic modeling of the BUT set-up data in terms of various straining. The results show the typical deformation pattern. One most important reason for favorable strength and more elongation increment that when the island contains is elongated, is for the reason that the shape and size make it more difficult for the sheet

Figure 11. Dispersion of plastic equivalent strain in I-M-DP600, matrix (a-d), and in the island (e-h) at edge region RVE for 5, 10, 15, and 20% engineering strain respectively

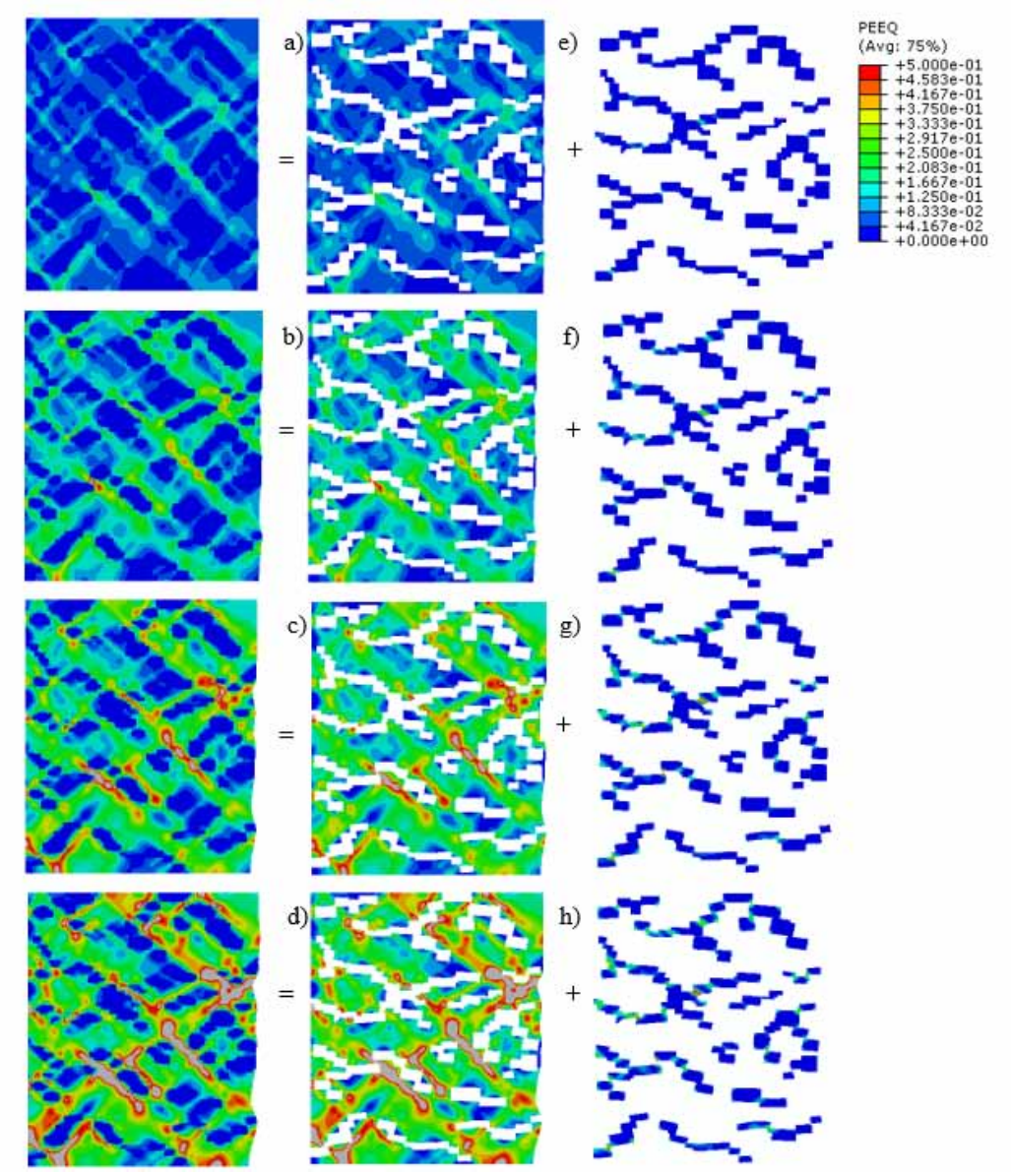

to deform without deforming the hard island contains, such as the geometrical dispersion restricts the plastic flow in the matrix resulting in a simultaneous rise in strength and elongation percentage. Saatcı and Salamci, 2017 showed that the relationship of increasing martensite VFs with hardness, and toughness on fractography studies after the tensile test was performed via. SEM in multiphase 15CrNiMo7 steel. Basu et al., 2018 established a correlation between hardness, VF of constituent phases, and morphological variation of multiphase 20MnMoNi55 Steel.

As it is shown the equivalent von-Mises stress in the island is much higher than the ferritic matrix but it is opposite for the plastic equivalent strain. Figures 11 and 12 depict the simulation of

Figure 12. Equivalent S, Mises stress distribution in I-M-DP600, matrix (a-d), and in the island (e-h) at edge region RVE for 5, 10, 15, and 20% engineering strain respectively

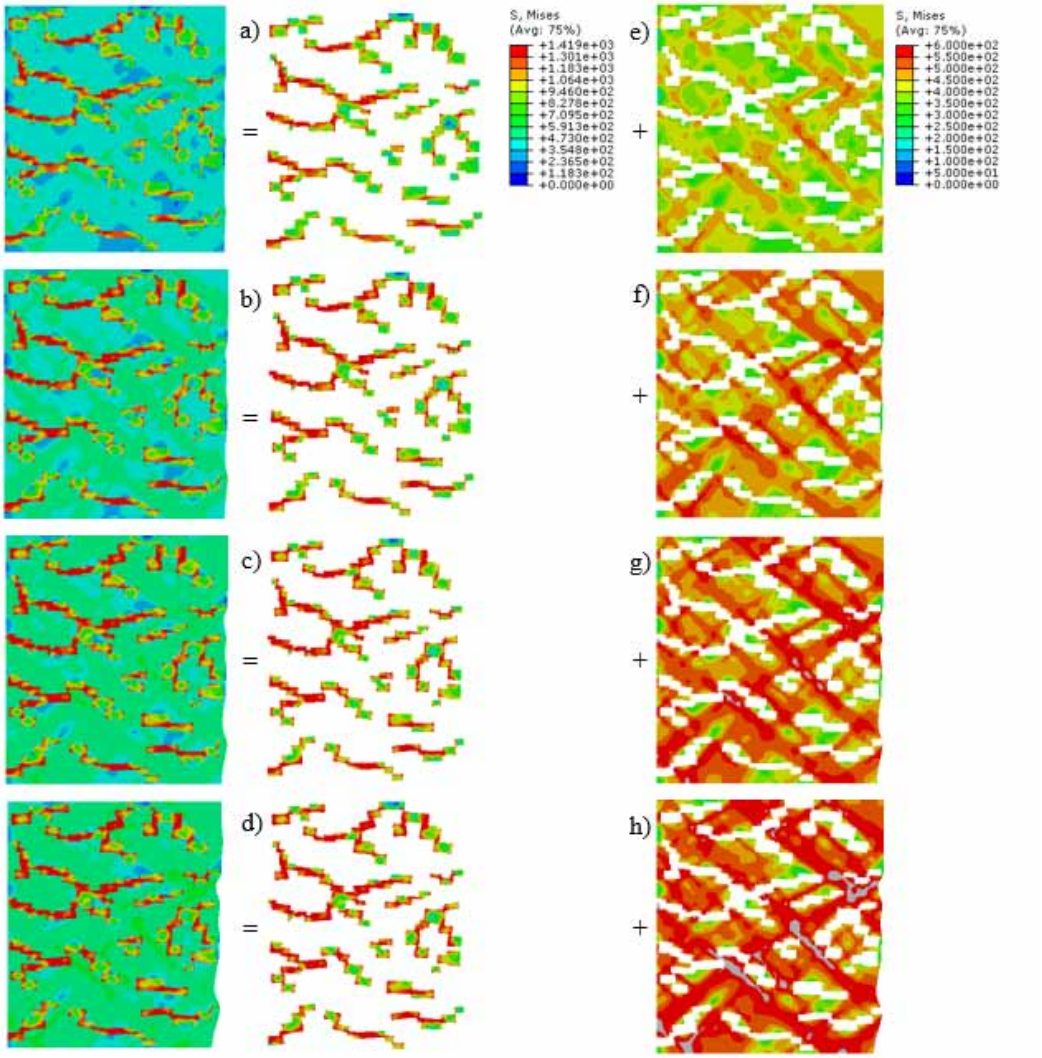

the RVE extracted from the edge region of the BUT setup. Figures 13and 14 depict the results of the RVE extracted from the centre region of the BUT set up as is shown in Fig. 5. From the comparisons, it can say that the plastic strain is increasing with an increase in overall strain and also it shows the relative deformation of centre and edge regions. The stress is more in the island phase. Also, it clearly shows that the plastic strain is more in the matrix.

The micro-mechanics based 2D RVE Finite Element (FE) models are capable to predict the complex deformation behavior, flow behavior, and ductility of I-M-DP steel from BUT test sample depending upon its position on the test specimen subjected to uniaxial tensile loading. It is significant that these studies that are compared the simulation results from 2D RVEs, 3D RVEs with practical bending under tension situation simulations. Automotive industries are frequently manufactured sheet metal from I-M-DP steels; therefore, all simulations directed in these recent studies are under plane

Figure 13. Dispersion of plastic strain in the matrix (a-d) & in the island (e-h) at center region RVE for 5, 10, 15, and 20% engineering strain respectively

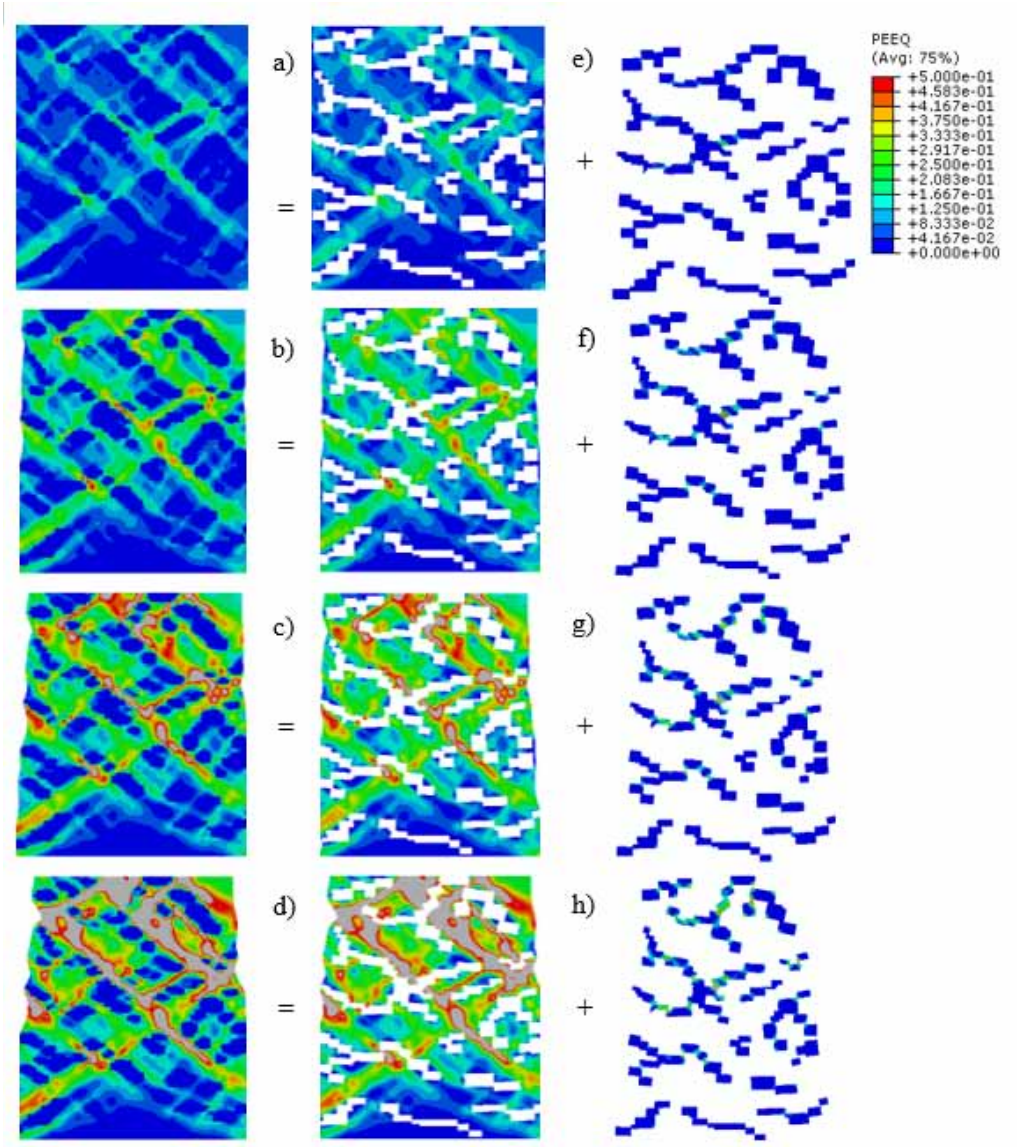

strain circumstances. Also, perfect bonding is believed between the two phases (I-M) during the load setting. However, it should be emphasized that, as compared to 3D RVEs, conducting 2D RVE-based modeling assuming plane-strain assumptions is more appropriate. Actuality, plane-strain estimates the effective properties including Z-axis stress-strain results. Therefore, the results are conventional as compared to BUT stress state.

During the time of deformation, localization of equivalent stress happens to be much larger in the islands than that in the matrix part. Stress concentration is getting increased while the radius/thickness value is getting increased. Stress concentration is also raised due to the restriction of deformation in the matrix by the island present in the matrix. An island that is in the matrix during the bending

Figure 14. Equivalent von Mises Stress distribution in I-M-DP600 (a-d) and matrix (e-h) at center region RVE for 5, 10, 15 and 20% engineering strain respectively

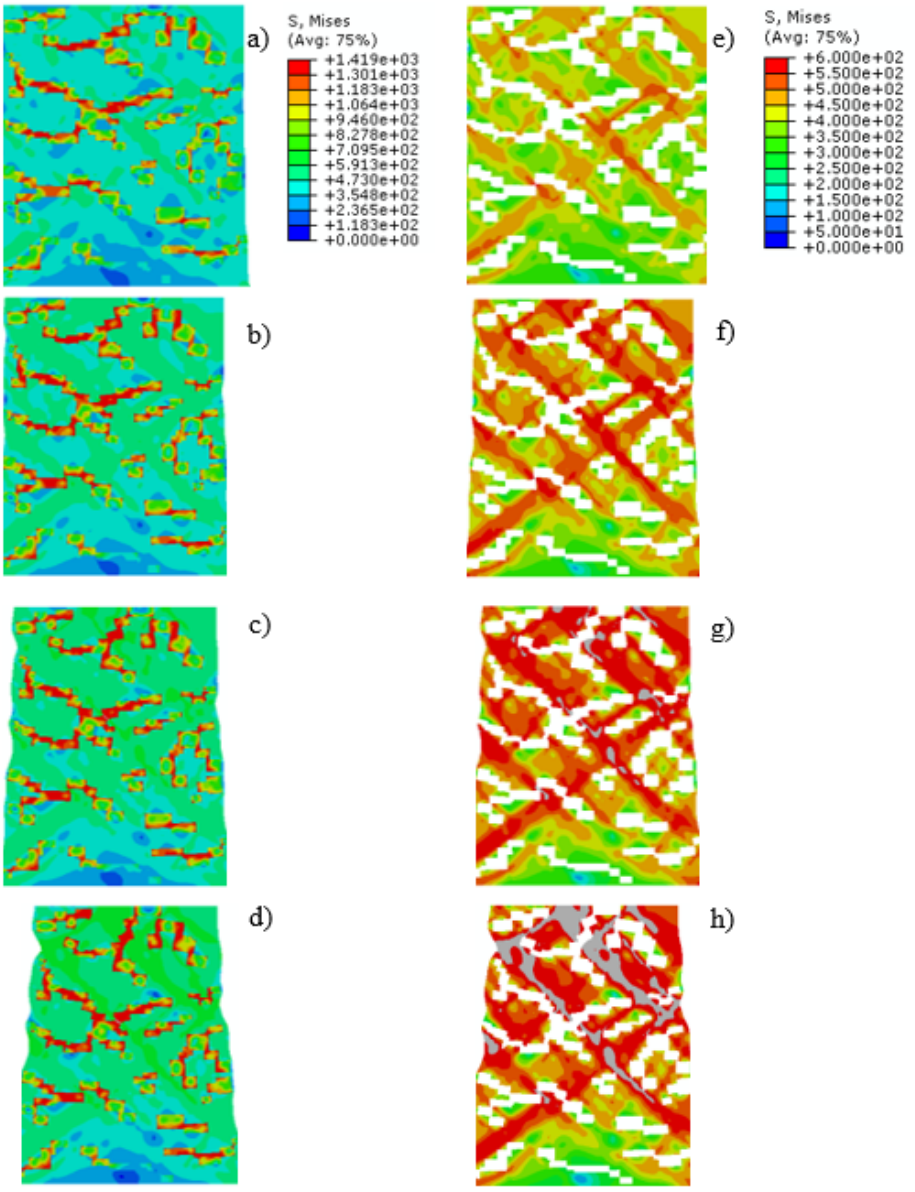

operation increases the strength of the sheet and high stress localization would happen which will cause ductile failure. Correspondingly for island-matrix steel, as deformation localization takes place in the matrix phase only and a higher strain hardening rate of matrix delays deformation localization, and hence elongation of overall island-matrix steel also increases. The RVEs model illustrates how various factors affect the predicted responses for the I-M-DP steels and presents the influence of the considered microstructure on the severe deformation responses at certain engineering strain rates.

3.3 Microscopic Simulation on 3D RVE

Three-dimensional RVE is the smallest volume of a microstructure over which the result is found that yields a better result for the representation of the whole. This apposite solution method is chosen for FE analysis of the typical microstructure of I-M-DP600 steel and it is addressed systematically. The volume fraction of matrix (76.5%) and island (23.5%) is arbitrarily dispersed in the 3D RVE of I-M-DP steel. For the entire FEA process of this RVE, the first step is to generate the required model for individual constituent components. Matrix and the island are allocated over the models. To perform the following RVE analysis, ABAQUS is used. Two constituents have been created, one set for the island and the other for matrix. Island has been allocated in 1880 cells and matrix allocated in 6120 cells. The sets are created with respect to geometry. The individual distinct constituent of matrix and island is shown in Fig 3. Distinct between the two phases of the I-M-DP steel i.e. matrix and island with respect to its phase fractions in the real microstructure is composed. A total of 64000 elements are created in the three dimensions computational domain. Whereas an 8-node brick, reduced integration, hourglass control (C3D8R) are used for discretization. Elastic-plastic FE analysis is carried out by using isotropic hardening parameters and dislocation based flow behavior of the material. Figure 15 shows the plastic equivalent strain distribution in matrix and island at 5, 10, 15, and 20% overall straining.

The von Mises stress distribution at 5, 10, 15, and 20% overall straining is shown in Fig. 16. It can be observed that the maximum von Mises stress is observed in the island regions having severe deformation regions. The maximum stress with a magnitude of 1419 MPa is at the island location. The study indicates that stress localization commences in the interfaces between the island and matrix, and hence increases rapidly around the martensite-islands. This is due to the high ductile plastic properties in the matrix and harder properties in the islands. In the matrix, on the other hand, the stress distribution tends to spread quickly in its neighborhood as the equivalent von Mises stress increases and features a distorted shape while the plastic strain goes up. Also, the high equivalent plastic strain distribution was mainly observed in the matrix adjacent to the neck in the form of shear bands.

During the progress of deformation, the localization of equivalent stress appears to be much larger around martensite islands than that in the matrix. Moreover, predominant stress localization regions are detected, apparently, near to the in between the matrix and islands. Similarly, 3D RVE analysis was done for better and more accurate flow results. The engineering stress-strain curve obtained from the 3D RVE is best fitted and almost nearer to the experimental curve. 3D RVE simulated stress-strain curve shows the instability or thinning stages for the material. On the other hand, the common situations of ductile failure modes of carbon steel material were established in the form of fracture instability and plastic collapse conditions (Rana et al., 2019c).

In this complex situation, the distribution of equivalent plastic equivalent strain in matrix and island is visualized, that strain partitioning occurs from the early stage of deformation in the 3D RVE after the matrix is yielded. References (Sun et al., 2009; Rana et al., 2020; Rana and Dey, 2021) showed that the centre of the tensile specimen fractured in a perpendicular manner, while inclined fracture was observed on both sides.

Recently I-M-DP steels are found in widespread applications in structural parts due to their excellent properties. Frames, crossbeams, vertical beams, side impact beams, and safety elements are often assembled with I-M-DP steels in automotive structures. Their applications in those parts are rapidly rising. Stress concentrators such as various joints are present in every structure. Such a stress concentration plays a crucial role in the early failure from a stress raiser. The simulated monotonic severe deformation situation is also compared with the experimental one and is also specified in Table 3. One exact radius and thickness ratio is chosen as per Wei et al., 2015. Forecasting of plastic strain localization in the RVEs does not necessitate any imperfection in geometries, preexisting void or damage, and failure principles, but it has been predicted well. Subsequently, the effects of alteration of such parameters are considered by systematic change of exact (obtained from the experimental result) parameters. The current study explored that the stress state of the sheet metal varies during

Figure 15. Equivalent plastic strain distribution in 3D RVE of I-M-DP 600 steel at 5, 10, 15, and 20% aggregate tensile straining

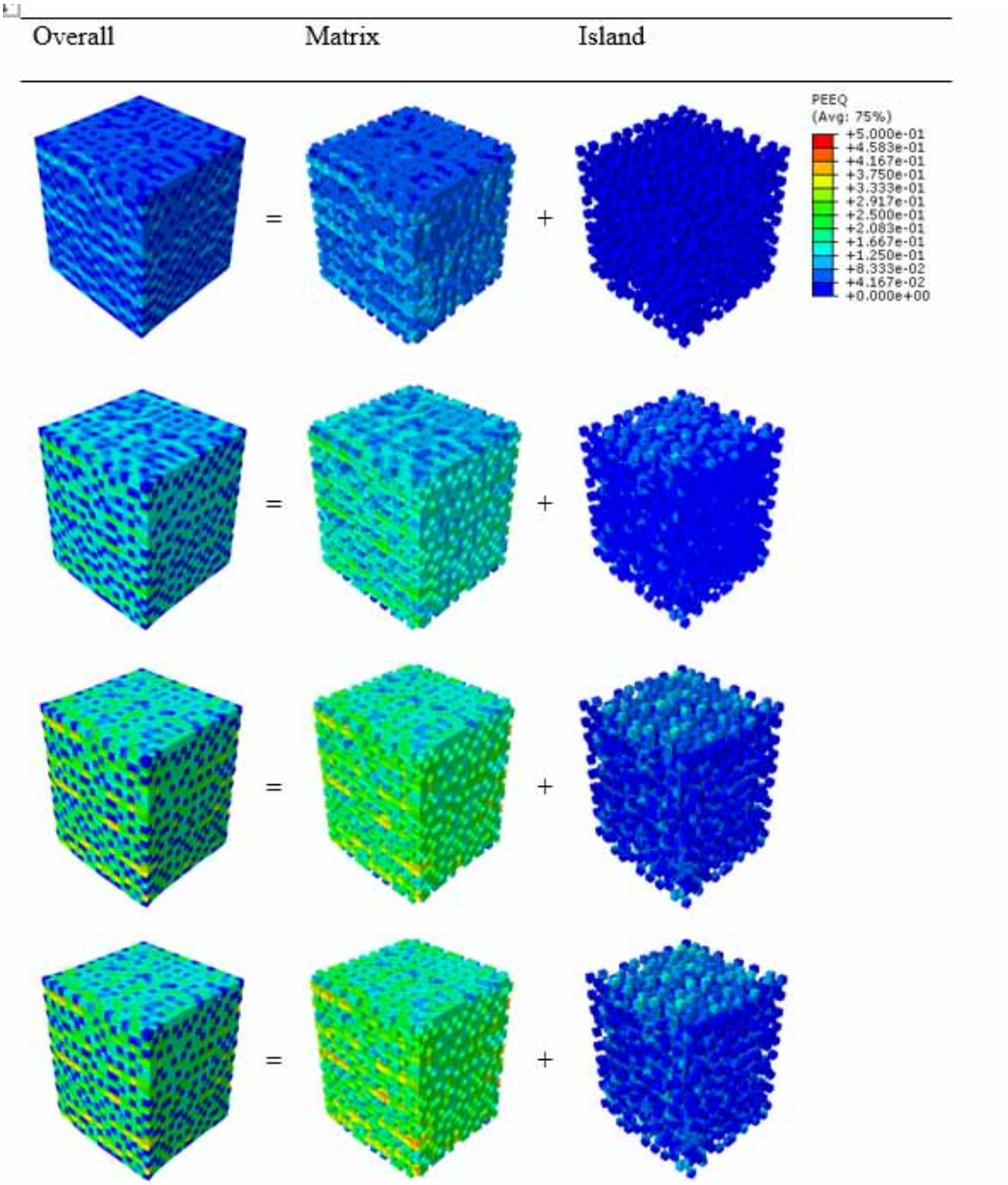

forming operation, and failure can be different in those cases. The main reason for these severe deformation patterns for all the cases is the deformation localization of plastic nature inside the matrix grows and coalesces, and eventually forms various sizes of deformation band. Islands lying inside the deformation band undergo incredible deformation. This creation of deformation bands results in concentrated bulky rate deformation merely within the deformation band, and thus forming an unloading consequence in other areas. Similarly, the stress state of the sheet metal varies during forming operation, and failure can be different in those cases. By engaging the classical local S, Mises plasticity without any damage law, it was concluded that failure mechanisms and loss of elongation of

Table 3. Comparison results of equivalent plastic strains and equivalent plastic stress from modeling and experiment

Factors	Conditions				
	BUT (equivalent plastic strains)			RVE (equivalent plastic stress)	
$(r/t)_{exp}$	6.7	11.7	17.5	S, Mises in overall	S, Mises in matrix
Experiment [26]	0.151	0.057	0.065	1416.67	608.78
$(r/t)_{sim.}$	6.7	16.7	20.8	S, Mises in overall	S, Mises in matrix
Simulation	0.1494	0.097	0.089	1419	609.6

Figure 16. Equivalent von Mises plastic stress dispersion in 3D RVE of I-M-DP 600 steel at 5, 10, 15, and 20% aggregate tensile straining

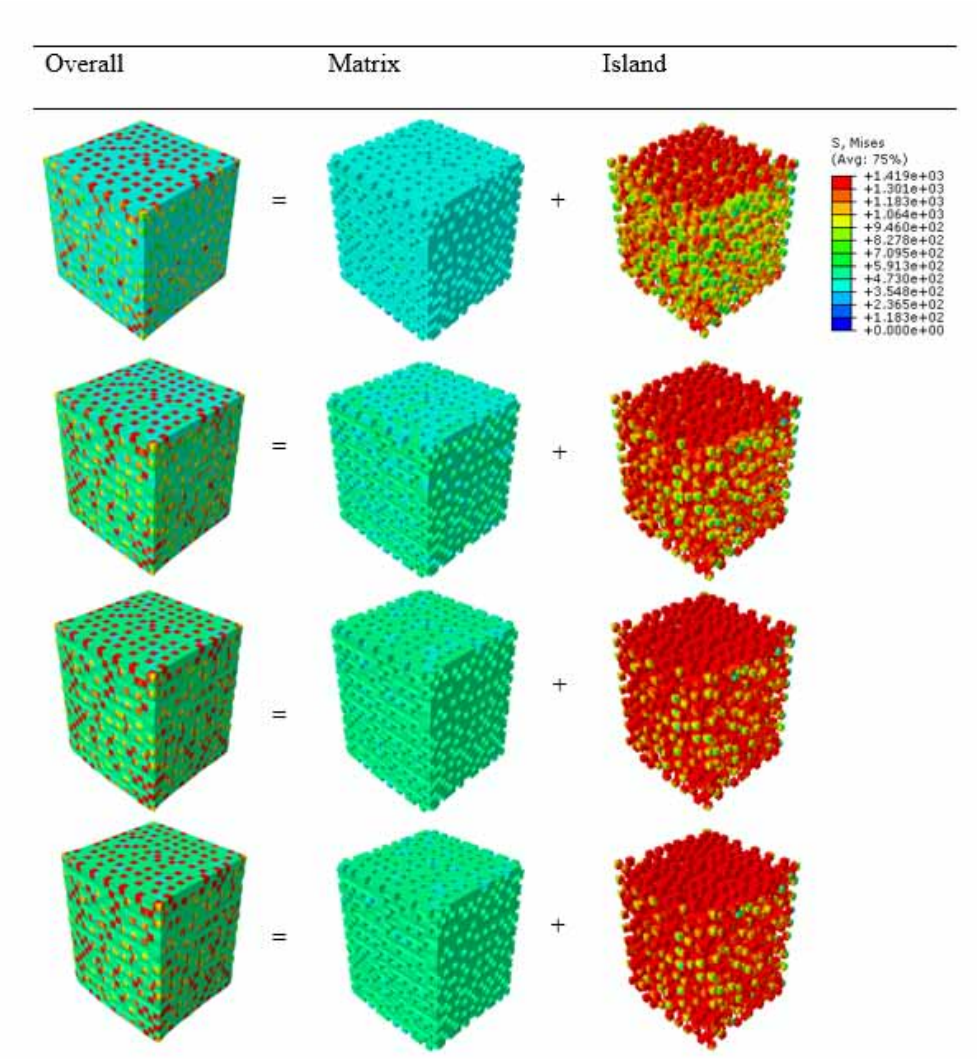

I-M-DP steels are owing to plastic strain localization state. However, in order to obtain an apparent representation of equivalent plastic strain dispersions, all virtual RVEs are shown a significant fallout from these systematic considerations. Hence, for simplicity, under monotonic load settings, boundary conditions are imposed in this study through prescribing constraints through Abaqus software. The predictions of current approaches closely agree with the experimental in terms of the micro and overall macroscopic response of the I-M-DP steel.

4. CONCLUSION

In this work, BUT modeling of I-M-DP steel is carried out for different r/t ratios. 2D and 3D RVEs of I-M-DP 600 steel are predicted well with the experimental result. These studies can be used to predict the deformation behavior, flow behavior, strain localization, and ductility of the forming test specimen. The severe deformation of I-M-DP steel is predicted in the form of plastic strain localization resulting from the incompatible deformation between the island and matrix phases. Based on the RVEs simulation results, the main conclusions are drawn as follows:

1. The results of BUT modeling along with microstructural 2D and 3D-RVE modeling show the fundamental mechanism of plastic flow, where the island impedes the material flow in the matrix. The results of micro-macro simulation are manifested as a well-matched characteristic with the experiment, which will facilitate this microstructure to be adapted for suitable applications in automobile components for example as a wheel disk material.
2. The dominant shear failure mode develops during uniaxial monotonic load settings on the island-matrix-dual phase steel. It should be noted that no specific failure criteria or imperfection are specified in the binary phases for the prediction of the overall uniaxial tensile flow behavior.
3. The plastic strain is localized by the incompatible plastic deformations accumulated in the binary constituent phases during the deformation process, and ultimately the failure of I-M-DP steel is perpetuated by the initial microstructural inhomogeneity. Here, inhomogeneity in the form of high deformation state accumulated areas of the RVE coalesced together.
4. Hence the effect of I-M-DP steel microstructure on the strain rate sensitivity is predicted by the micro-macro modeling. To attain the needs of steel companies and automobile designers, the components requirements of automobile structure can be maintained, and required materials for the intended application can be produced by changing the characteristics of I-M-DP steel.

REFERENCES

Ajmal, M., Tindyala, M. A., & Priestner, R. (2009). Effect of controlled rolling on the martensitic hardenability of dual phase steel. *International Journal of Minerals Metallurgy and Materials*, *165-169*(2), 165–169. Advance online publication. doi:10.1016/S1674-4799(09)60028-5

Basu, P., Acharyya, S. K., & Sahoo, P. (2018). A correlation study between mechanical properties and morphological variation of 20MnMoNi55 steel. *Silicon*, *10*(4), 1257–1264. doi:10.1007/s12633-017-9598-x

Belgasam, T. M., & Zbib, H. M. (2017). Microstructure Optimization of Dual-Phase Steels Using a Representative Volume Element and a Response Surface Method: Parametric Study. *Metallurgical and Materials Transactions. A, Physical Metallurgy and Materials Science*, *48*(12), 6153–6177. doi:10.1007/s11661-017-4351-z

Belgasam, T. M., & Zbib, H. M. (2018). Key factors influencing the energy absorption of dual-phase steels: Multiscale material model approach and microstructural optimization. *Metallurgical and Materials Transactions. A, Physical Metallurgy and Materials Science*, *49*(6), 2419–2440. doi:10.1007/s11661-018-4563-x

Carden, W. D., Geng, L. M., Matlock, D. K., & Wagoner, R. H. (2002). Measurement of springback. *International Journal of Mechanical Sciences*, *44*(1), 79–101. doi:10.1016/S0020-7403(01)00082-0

Dai, J., Meng, Q., & Zheng, H. (2020). High-strength dual-phase steel produced through fast-heating annealing method. *Results Mater*, *5*, 100069. doi:10.1016/j.rinma.2020.100069

Darabi, A. C., Chamani, H. R., Kadkhodapour, J., Anaraki, A. P., Alaie, A., & Ayatollahi, M. R. (2017). Micromechanical analysis of two heat-treated dual phase steels: DP800 and DP980. *Mechanics of Materials*, *110*, 68–83. doi:10.1016/j.mechmat.2017.04.009

Das, B., Paul, S. K., Singh, A., Arora, K. S., & Shome, M. (2020). The effect of thickness variation and pre-strain on the cornering fatigue life prediction of a DP600 steel wheel disc. *International Journal of Fatigue*, *139*, 105799. doi:10.1016/j.ijfatigue.2020.105799

Krajewski, S., & Nowacki, J. (2014). Dual-phase steels microstructure and properties consideration based on artificial intelligence techniques. *Archives of Civil and Mechanical Engineering*, *14*(2), 278–286. doi:10.1016/j.acme.2013.10.002

Li, K. P., Carden, W. P., & Wagoner, R. H. (2002). Simulation of springback. *International Journal of Mechanical Sciences*, *44*(1), 103–122. doi:10.1016/S0020-7403(01)00083-2

Liedl, U., Traint, S., & Werner, E. A. (2002). An unexpected feature of the stress–strain diagram of dual-phase steel. *Computational Materials Science*, *25*(1-2), 122–128. doi:10.1016/S0927-0256(02)00256-2

Paul, S. K. (2013). Effect of martensite volume fraction on stress triaxiality and deformation behavior of dual phase steel. *Materials & Design*, *50*, 782–789. doi:10.1016/j.matdes.2013.03.096

Paul, S. K. (2013). Real microstructure based micromechanical model to simulate microstructural level deformation behavior and failure initiation in DP 590 steel. *Materials & Design*, *44*, 397–406. doi:10.1016/j.matdes.2012.08.023

Paul, S. K., & Kumar, A. (2012). Micromechanics based modeling to predict flow behavior and plastic strain localization of dual phase steels. *Computational Materials Science*, *63*, 66–74. doi:10.1016/j.commatsci.2012.05.061

Paul, S. K., & Mukherjee, M. (2014). Determination of bulk flow properties of a material from the flow properties of its constituent phases. *Computational Materials Science*, *84*, 1–12. doi:10.1016/j.commatsci.2013.11.039

Paul, S. K., Stanford, N., & Hilditch, T. (2015). Effect of martensite volume fraction on low cycle fatigue behaviour of dual phase steels: Experimental and microstructural investigation. *Materials Science and Engineering A*, *638*, 296–304. doi:10.1016/j.msea.2015.04.059

Paul, S. K., Stanford, N., & Hilditch, T. (2015). Effect of martensite morphology on low cycle fatigue behaviour of dual phase steels: Experimental and microstructural investigation. *Materials Science and Engineering A*, *644*, 53–60. doi:10.1016/j.msea.2015.07.044

Ramazani, A., Mukherjee, K., Quade, H., Prahl, U., & Bleck, W. (2013). Correlation between 2D and 3D flow curve modelling of DP steels using a microstructure-based RVE approach. *Materials Science and Engineering A*, *560*, 129–139. doi:10.1016/j.msea.2012.09.046

Rana, A. K., Acharyya, S. K., & Dhar, S. (2019c). A simplified procedure to prediction of ductile failure modes of a SA333 Gr. 6 carbon steel pipe: Fracture instability and Plastic collapse condition. *Materials Today: Proceedings*, *18*, 2893–2902. doi:10.1016/j.matpr.2019.07.158

Rana, A. K., & Dey, P. P. (2021). Predicting Plastic Flow Behavior, Failure mechanisms and severe deformation Localisation of Dual-Phase Steel using RVE simulation. *International Journal of Automotive and Mechanical Engineering*, *18*(1), 8601–8611. doi:10.15282/ijame.18.1.2021.19.0654

Rana, A. K., Paul, S. K., & Dey, P. P. (2018). Effect of martensite volume fraction on strain partitioning behavior of dual phase steel. *Physical Mesomechanics*, *21*(4), 333–340. doi:10.1134/S1029959917040070

Rana, A. K., Paul, S. K., & Dey, P. P. (2019a). Effect of martensite volume fraction on cyclic plastic deformation behavior of dual phase steel: Micromechanics simulation study. *Journal of Materials Research and Technology*, *8*(5), 3705–3712. doi:10.1016/j.jmrt.2019.06.022

Rana, A. K., Paul, S. K., & Dey, P. P. (2019b). Stress field in an isotropic elastic solid containing a circular hard or soft inclusion under uniaxial tensile stress. *Materials Today: Proceedings*, *11*, 657–666. doi:10.1016/j.matpr.2019.03.024

Rana, A. K., Paul, S. K., & Dey, P. P. (2020). Effect of individual phase properties and volume fractions on the strain partitioning, deformation localization and tensile properties of DP steels. *Sadhana*, *45*(1), 235. doi:10.1007/s12046-020-01438-7

Saatcı, T., & Salamci, E. (2017). The effect of microstructure on tensile strength of high martensite dual-phase steels. *Kovove Mater*, *55*(05), 333–342. doi:10.4149/km_2017_5_333

Samei, J., Green, D. E., & Golovashchenko, S. (2014). Analysis of failure in dual phase steel sheets subject to electrohydraulic forming. *Journal of Manufacturing Science and Engineering*, *136*(5), 051010. doi:10.1115/1.4027940

Sirinakorn, T., Wongwises, S., & Uthaisangsuk, V. (2014). A study of local deformation and damage of dual phase steel. *Materials & Design*, *64*, 729–742. doi:10.1016/j.matdes.2014.08.009

Sodjit, S., & Uthaisangsuk, V. (2012). Microstructure based prediction of strain hardening behavior of dual phase steels. *Materials & Design*, *41*, 370–379. doi:10.1016/j.matdes.2012.05.010

Sun, X., Choi, K. S., Liu, W. N., & Khaleel, M. A. (2009). Predicting failure modes and ductility of dual phase steels using plastic strain localization. *International Journal of Plasticity*, *25*(10), 1888–1909. doi:10.1016/j.ijplas.2008.12.012

Uthaisangsuk, V., Prahl, U., & Bleck, W. (2009). Stretch-flangeability characterisation of multiphase steel using a microstructure based failure modelling. *Computational Materials Science*, *45*(3), 617–623. doi:10.1016/j.commatsci.2008.06.024

Uthaisangsuk, V., Prahl, U., & Bleck, W. (2011). Modelling of damage and failure in multiphase high strength DP and TRIP steels. *Engineering Fracture Mechanics*, *78*(3), 469–486. doi:10.1016/j.engfracmech.2010.08.017

Wagoner, R. H., & Li, M. (2005). Advances in springback. AIP Conference Proceedings, 778, 209-214. doi:10.1063/1.2011219

Wang, J. F., Wagoner, R. H., Matlock, D. K., & Barlat, F. (2005). Anticlastic curvature in draw-bend springback. *International Journal of Solids and Structures*, *42*(5-6), 1287–1307. doi:10.1016/j.ijsolstr.2004.08.017

Wei, X., Asgari, S. A., Wang, J. T., Rolfe, B. F., Zhu, H. C., & Hodgson, P. D. (2015). Micromechanical modelling of bending under tension forming behaviour of dual phase steel 600. *Computational Materials Science*, *108*, 72–79. doi:10.1016/j.commatsci.2015.06.012

Zhuang, X. C., Xu, C., Wang, T., & Zhao, Z. (2014). Failure mode and ductility of dual phase steel with edge crack. *Procedia Engineering*, *81*, 766–771. doi:10.1016/j.proeng.2014.10.074

Amit Kumar Rana received a Bachelor of Engineering in Mechanical Engineering from Jalpaiguri Government Engineering College. He received Master of Engineering in Mechanical Engineering from Jadavpur University, Kolkata. He received his PhD in Mechanical Engineering from Indian Institute of Engineering Science and Technology, Shibpur, Howrah-711103, India. Presently he is an Assistant Professor in the Department of Mechanical Engineering of The ICFAI University Tripura, Agartala-799210, India. His area of research interest is Computational mechanics/ FEM modelling and simulation/Computational plasticity/Micromechanical modelling/Mechanics of materials and Design Engineering.